Reversible Binuclear Cu(II) Complex Formation in a New Sonogel−Cryptand Hybrid Material

Manuel G. Basallote,*,† Eduardo Blanco,‡ María J. Fernández-Trujillo,† M. Angeles Máñez,† and Milagrosa Ramírez del Solar‡

Departamento de Ciencia de los Materiales e Ingeniería Metalúrgica y Química Inorgánica and Departamento de Física de la Materia Condensada, Facultad de Ciencias, Universidad de Cádiz, Apartado 40, 11510-Puerto Real (Cádiz), Spain

Received July 3, 2001. Revised Manuscript Received September 24, 2001

New hybrid materials are obtained by embedding Cu(II) complexes of the open-chain triethylenetetraamine ligand (*tren*) or a related binucleating cryptand containing two *tren* subunits in sonogel matrixes prepared from tetraethoxysilane (TEOS) or methyltriethoxysilane (MTEOS). The effectiveness of trapping depends on both the matrix and the nature of the complex. The chemical behavior and textural parameters of the different samples are explained according to a textural model with three different types of sites for trapping. The most promising samples for sensing purposes are TEOS-based silica sonogel matrixes containing the binuclear Cu(II) cryptate, where reversible reactions with small ions (H^+, Cu^{2+}, N_3^-) take place in a way similar to that observed in solution. However, successive reaction cycles lead to the partial loss of the trapped cryptand. Leaching becomes less important when the sonogel is prepared from TEOS and a salt of the protonated cryptand. In this case, the texture of the matrix is more suitable for cryptand trapping, and treatment with solutions containing Cu^{2+}, N_3^-, or H^+ leads to a larger number of reversible complex formation−decomposition processes.

Introduction

The preparation of sol−gel materials incorporating metal complexes and other dopants into the network is a field of great interest[1] because of their relevance to electrochemical[2−4] and optical[5−11] sensing, catalysis,[12−17] gas separation,[18] and other applications.[19−21] Trapping of a metal complex into the sol−gel matrix can be achieved by simply adding the complex to a fresh silica sol or, more efficiently, by forcing the formation of covalent bonds between the matrix and one or more ligands.[22−24] In any case, a hybrid organic−inorganic material results in which the complexes or the ligands can act either as network modifiers or as network formers. One of the major problems associated with the study of these materials is the lack of knowledge about the way in which sol−gel trapping modifies the properties of the metal complexes. As the environment of the complex in a sol−gel matrix is very different from that in solution, it is possible that chemical properties such as the thermodynamics and kinetics of reactions are modified.[9] Thus, we consider that the use of sol−gel materials incorporating metal complexes as sensors requires the previous determination of the way in which the chemical reactivity of the complexes is modified upon trapping.

In this work, we have chosen to investigate the Cu(II) complexes of the large cryptand L, which contains two

* Author to whom correspondence should be addressed.
† Departamento de Ciencia de los Materiales e Ingeniería Metalúrgica y Química Inorgánica.
‡ Departamento de Física de la Materia Condensada.

(1) Gill, I.; Ballesteros, A. *TIBTECH* **2000**, *18*, 282.
(2) Aranda, P.; Jiménez-Morales, A.; Galván, J. C.; Casal, B.; Ruiz-Hitzky, E. *J. Mater. Chem.* **1995**, *5*, 817.
(3) Rabinovich, L.; Gun, J.; Tsionsky, M.; Lev, O. *J. Sol-Gel Sci. Technol.* **1997**, *8*, 1077.
(4) Hidalgo, J. L.; Cordero, M.; Naranjo, I.; Blanco, E.; Esquivias, L. ES Patent P200100556, 2001.
(5) Fu, L.; Zhang, H.; Wang, S.; Meng, Q.; Yang, K.; Ni, J. *J. Sol-Gel Sci. Technol.* **1999**, *15*, 49.
(6) McCraith, B. D.; McDonagh, C.; Mcevoy, A. K.; Butler, T.; O'Keeffe, G.; Murphy, V. *J. Sol-Gel Sci. Technol.* **1997**, *8*, 1053.
(7) Bendavid, O.; Shafir, E.; Gilath, I.; Prior, Y.; Avnir, D. *Chem. Mater.* **1997**, *9*, 2255.
(8) Murtagh, M. T.; Shahriari, M. R.; Krihak, M. *Chem. Mater.* **1998**, *10*, 3862.
(9) Hartnett, A. M.; Ingersoll, C. M.; Baker, G. A.; Bright, F. V. *Anal. Chem.* **1999**, *71*, 1215.
(10) Leventis, N.; Elder, I. A.; Rolison, D. R.; Anderson, M. L.; Merzbacher, C. I. *Chem. Mater.* **1999**, *11*, 2837.
(11) Pandey, S.; Baker, G. A.; Kane, M. A.; Bonzagni, N. J.; Bright, F. V. *Chem. Mater.* **2000**, *12*, 3547.
(12) Louloudi, M.; Deligiannakis, Y.; Hadjiliadis, N. *Inorg. Chem.* **1998**, *37*, 6847.
(13) Hüsing, N.; Reisleer, E.; Zink, J. I. *J. Sol-Gel Sci. Technol.* **1999**, *15*, 57.
(14) Cauqui, M. A.; Rodríguez-Izquierdo, J. M. *J. Non-Cryst. Solids* **1992**, *147−148*, 724.
(15) Bodsgard, B. R.; Burstyn, J. N. *Chem. Commun.* **2001**, 647.
(16) Badjic, J. D.; Kostic, N. M. *Chem. Mater.* **1999**, *11*, 3671.
(17) Murphy, E. F.; Schmid, L.; Bürgi, T.; Maciejewski, M.; Baiker, A.; Günther, D.; Schneider, M. *Chem. Mater.* **2001**, *13*, 1296.
(18) Kuraoka, K.; Chujo, Y.; Yazawa, T. *Chem. Commun.* **2000**, 2477.
(19) Lin, H. P.; Cheng, Y. R.; Mou, C. Y. *Chem. Mater.* **1998**, *10*, 3772.
(20) Adeogun, M. J.; Hay, J. N. *Chem. Mater.* **2000**, *12*, 767.
(21) Galván, J. C.; Aranda, P.; Amarilla, J. M.; Casal, B.; Ruiz-Hitzky, E. *J. Mater. Chem.* **1993**, *3*, 687.
(22) Kloster, G. M.; Taylor, C. M.; Watton, S. P. *Inorg. Chem.* **1999**, *38*, 3954.
(23) Dubois, G.; Corriu, R. J. P.; Reyé, C.; Brandès, S.; Denat, F.; Guilard, R. *Chem. Commun.* **1999**, 2283.
(24) Tien, P.; Chau, L. K. *Chem. Mater.* **1999**, *11*, 2141.

10.1021/cm0111635 CCC: $22.00
Published on Web 01/26/2002

triethylenetetraamine (*tren*) subunits separated by three *m*-xylyl spacers (see below).

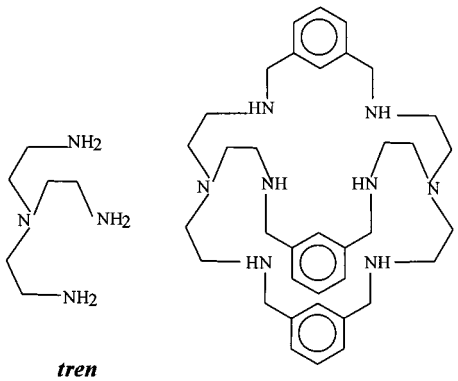

This kind of ligand, as well as its metal complexes, has been shown to be useful for optical sensing because of its selective complexation with different anions and neutral molecules.[25,26] Previous stability and structural work with this and related ligands has shown that binuclear Cu_2L^{4+} and $Cu_2L(OH)^{3+}$ complexes are formed by coordination of one Cu(II) to each *tren* subunit.[27,28] More recently, some of us have shown that the formation of stable ternary Cu−L−X complexes (X = SCN^-, N_3^-) occurs rapidly in solution, whereas the total decomposition of the complexes upon addition of an excess of acid is also rapid.[29] The results in the present work show clearly that these large binuclear complexes can be trapped into sol−gel matrixes by the use of ultrasound, i.e., without the need for covalent bonding to the matrix. For comparative purposes, we have also prepared sol−gel materials containing Cu(II) complexes of the related nonmacrocyclic *tren* ligand. Although some binuclear Cu(II) complexes have been reported for *tren* and related ligands,[30,31] the stability data indicate that the major species in solution are mononuclear complexes.[27]

Experimental Section

The reagents tris-(2-aminoethyl)amine (*tren*), isophthalaldehyde, NaN_3, and $Cu(NO_3)_2{\cdot}6H_2O$ were obtained from Aldrich; tetraethoxysilane (TEOS) from Merck; methyltriethoxysilane (MTEOS) from ABCR; and formamide, ethanol, and the phosphate buffer from Panreac. The cryptand L was prepared from *tren* and isophthalaldehyde using the literature procedure[28] and was available as the L·8HBr salt from a previous work.[29] Solutions containing the binuclear Cu−L complexes were prepared by dissolving the required amounts of L and $Cu(NO_3)_2{\cdot}6H_2O$ in a small volume of ethanol, in such a way that the resulting solutions can be considered almost saturated. For the case of the nonmacrocyclic *tren* ligand, the solutions to be used in the sol−gel preparations were also obtained by dissolving *tren* and $Cu(NO_3)_2{\cdot}6H_2O$ (1:1 molar ratio) in ethanol. Visible spectra were obtained with a Perkin-Elmer Lambda 3B spectrophotometer.

Preparation of the Sonogels. For the A sample set, a pure inorganic matrix was prepared by the hydrolysis and polycondensation of TEOS, using a H_2O/TEOS molar ratio (R_w) of 3 in the presence of HNO_3 (pH = 1) for an acid-catalyzed sol−gel process. Formamide was added as a drying control chemical additive (DCCA)[32] in a TEOS/formamide molar ratio (R_F) of 3. Reactions were promoted with high-power ultrasound by the procedure known as sonocatalysis.[33,34] Complex-doped samples were obtained after addition of the solutions of Cu−L or Cu−*tren* complexes in ethanol to the resulting silica sol, the amount of solution being that required to achieve a 1:1 volume ratio. After mixing, the liquids were transferred to sealed PVC cuvettes and left to gel in an oven at 40 °C. After 1 week of aging and another week of drying in the unsealed containers, monolithic pieces (15 × 5 × 5 mm) of stable samples resulted. The samples containing the Cu−L complex are referred as A-CuL and those containing Cu−*tren* as A-Cu*tren*. For a more complete interpretation of the results, two more A samples were prepared: an undoped A matrix (no metal complex) and a sample doped with L alone (A-L sample). They were prepared in the same way as those containing the metal complexes, except that ethanol was replaced by a pH 7 phosphate buffer that is a better ligand solvent. Monolithic pieces with suitable mechanical properties are obtained by this procedure. Analogous problems of shrinkage and cracking during the preparation of xerogels containing trapped crown ethers have been reported.[2,21]

A similar procedure was followed for the preparation of the B sample set, using MTEOS as the precursor for a hybrid organic−inorganic matrix, but with a water molar ratio of R_w = 2 because of the lower number of RO− groups than in MTEOS in TEOS. Therefore, B-CuL and B-Cu*tren* monolithic samples resulted after doping with complex solutions, gelling, aging, and drying. Because of the existence of terminating Si−CH_3 groups and the lower O-bonding number of MTEOS than TEOS, the structure of this matrix is expected to be more open because of the lower reticulation degree achievable. In contrast, low-porosity ormosils should be expected when the nonhydrolyzable group in the precursor is a long organic chain. In this case, the globular-shaped organic phase fills the cavities (pores) of the inorganic network giving rise to a significant reduction in porosity.

Tests Performed on Hybrid Sonogels. The samples prepared according to the procedure described above were tested by checking their ability to react with acids, Cu^{2+} and N_3^-. To avoid any possible interference caused by weakly trapped complex molecules, the monoliths were first washed three times with distilled water over 24 h, which leads to reproducible absorption spectra.

Once washed, the samples were immersed in aqueous solutions containing the desired acid or salt. Under these conditions, the color changes of the sonogels can be used to monitor the reaction of the trapped complexes. Once the color change for a given reaction was completed, as confirmed by a stable absorption spectrum, the samples were washed again before being immersed in a new solution of acid or salt. In

(25) (a) Fabbrizzi, L.; Pallavicini, P.; Perotti, A.; Parodi L.; Taglietti, A. *Inorg. Chim. Acta* **1995**, *238*, 5. (b) Fabbrizzi, L.; Francese, G.; Licchelli; Perotti, A.; Taglietti, A. *Chem. Commun.* **1997**, 581. (c) Fabbrizzi, L.; Faravelli, I.; Francese, G.; Licchelli, M.; Perotti, A.; Taglietti, A. *Chem. Commun.* **1998**, 971.

(26) (a) Mason, S.; Clifford, T.; Seib, L.; Kuczera, K.; Bowman-James, K. *J. Am. Chem. Soc.* **1998**, *120*, 8899. (b) Morgan, G.; McKee, V.; Nelson, J. *J. Chem. Soc., Chem. Commun.* **1995**, 1649. (c) Maubert, B. M.; Nelson, J.; McKee, V.; Town, R. M.; Pál, I. *J. Chem. Soc., Dalton Trans.* **2001**, 1395.

(27) Smith, R. M.; Martell, A. E.; Motekaitis, R. J. *NIST Critical Stability Constants of Metal Complexes Database*; National Institute of Standards and Technology: Gaithersburg, MD, 1993.

(28) Menif, R.; Reibenspies, J.; Martell, A. E. *Inorg. Chem.* **1991**, *30*, 3446.

(29) Basallote, M. G.; Durán, J.; Fernández-Trujillo, M. J.; Máñez, M. A. *J. Chem. Soc., Dalton Trans.* **1999**, 3817.

(30) Dittler-Klingemann, A. M.; Orvig, C.; Hahn, F. E.; Thaler, F.; Hubbard, C. D.; Van Eldik, R.; Schindler, S.; Fábián, I. *Inorg. Chem.* **1996**, *35*, 7798.

(31) Thaler, F.; Hubbard, C. D.; Heinemann, F. W.; Van Eldik, R.; Schindler, S.; Fábián, I.; Dittler-Klingemann, A. M.; Hahn, F. E.; Orvig, C. *Inorg. Chem.* **1998**, *37*, 4022.

(32) Hench, L. In *Science of Ceramic Chemical Processing*; Hench, L., Ulrich, D. R., Eds.; Wiley: New York, 1986; p 52−64.

(33) Esquivias, L.; Zarzycki, J. In *Ultrastructure Processing of Ceramic, Glasses and Composites*; Mackenzie, J. D., Ulrich, D. R., Eds.; Wiley: New York, 1988; pp 255−270.

(34) Ramírez-del-Solar, M.; de la Rosa-Fox, N.; Esquivias, L.; Zarzycki, J. *J. Non-Cryst. Solids* **1990**, *121*, 40.

general, the following protocol of reactions was followed: (1) reaction of sonogels containing Cu−L or Cu−*tren* complexes with HNO_3 excess, (2) treatment with 0.1 M $Cu(NO_3)_2$ solution, (3) reaction with 0.1 M NaN_3, and (4) reaction with HNO_3, and the cycle was repeated if regeneration of the trapped metal complexes upon treatment with Cu(II) solution was observed. For the case of the hybrid materials prepared from L alone, the reaction sequence was started with the addition of the Cu(II) solution.

Some representative monoliths were selected for a porosity study that was carried out by making nitrogen physisorption experiments at 77 K with a Carlo Erba Sorptomatic 1900 instrument.

Results and Discussion

Summary of the Solution Behavior of the Cu−L and Cu−*tren* Complexes. Both ligands L and *tren* contain several nitrogen donors that are able to occupy several coordination sites about Cu(II). Because of the special arrangement of the four donor groups of *tren*, a pentacoordinate trigonal bipyramidal geometry about Cu(II) is favored, with coordination being completed with one monodentate ligand (a water molecule in the absence of better ligands).[35] Thus, formation of the Cu−*tren* complex in aqueous solution can be represented by eq 1, whereas reaction with a monodentate ligand as N_3^- is given by eq 2.

$$Cu^{2+} + tren \rightarrow Cu(tren)(H_2O)^{2+} \quad (1)$$

$$Cu(tren)(H_2O)^{2+} + N_3^- \rightarrow Cu(tren)(N_3)^+ \quad (2)$$

Equations 1and 2 represent pH-dependent processes because, in solution, there is a competition between the metal ion and H^+ for binding to the ligand, so that complex decomposition (the reverse processes) occurs upon addition of acid to a solution of the complex. The extreme lability of the hexaaquo Cu^{2+} ions is well-known, and so, eq 1 is a rapid process. Although the change from an octahedral to a trigonal bipyramidal structure reduces the lability of Cu(II) in $Cu(tren)(H_2O)^{2+}$, reactions in eq 2 are still rapid and are also completed in fractions of a second at room temperature using concentrations typical of kinetic studies (10^{-4}–10^{-2} M).[36,37]

For the case of L, each *tren* subunit can accommodate one Cu(II) ion in a pentacoordinate environment, and complex formation is a two-stage process (eqs 3 and 4).[28]

$$Cu^{2+} + L \rightarrow CuL^{2+} \quad (3)$$

$$CuL^{2+} + Cu^{2+} \rightarrow Cu_2L^{4+} \quad (4)$$

For this kind of binucleating ligand, the electrostatic repulsion between the close Cu(II) centers in Cu_2L^{4+} causes a high tendency to form a bridge between them using a negatively charged X^- ligand ($X^- = OH^-$, SCN^-, or N_3^-), which leads to stable $Cu_2L(X)^{3+}$ complexes.[28,29,38] Although one would expect that electrostatic repulsion causes a decrease in the rate of coordination of the second metal ion, we have shown that the *tren* subunits in L behave independently and the kinetics of eqs 3 and 4 is statistically controlled, i.e., the rate of entry of the first metal ion into the cryptand cavity is twice the rate corresponding to the entry of the second ion.[29] Statistical kinetics was also observed for complex decomposition upon addition of an excess of acid (reverse of eqs 3 and 4). Although a detailed kinetic study could not be carried out, the reaction of X-bridged binuclear complexes with a different anionic ligand to change the nature of the bridge (eq 5) is also rapid. Addition of an excess of acid to solutions of $Cu_2L(X)^{3+}$ complexes leads in all cases to complete complex decomposition (eq 6) in a rapid process whose kinetics is only slightly dependent on the nature of X^-.[39]

$$Cu_2L(X)^{3+} + Y^- \rightarrow Cu_2L(Y)^{3+} + X^- \quad (5)$$

$$Cu_2L(X)^{3+} + 6H^+ \rightarrow 2Cu^{2+} + H_6L^{6+} + X^- \quad (6)$$

Chemical Reactivity of the Trapped Complexes. The visible spectra of sonogels containing the Cu−L or Cu−*tren* complexes are similar to those of solutions containing the corresponding complexes, which indicates that the coordination environment is maintained upon trapping. However, for samples of the B series containing the Cu−*tren* complex, the washing protocol led to complete discoloration of the samples, with disappearance of the bands typical of Cu−*tren* complexes.[36,37] All attempts to regenerate the spectrum of unwashed monoliths by treatment with Cu(II), *tren*, and Cu−*tren* solutions were unsuccessful because subsequent washing with distilled water always caused complete discoloration. These results clearly indicate that B-Cu*tren* samples contain only weakly trapped complex molecules that are easily released upon contact with an aqueous solution, which is consistent with the lower trapping ability of the hybrid network caused by the more open structure of the material.

In contrast, the A-Cu*tren* samples were not completely discolored upon washing, and the bands typical of the complex were observed even after 10 successive washing cycles. Surprisingly, although the complex decomposes rapidly in acidic solutions, these monoliths remain colored after treatment with commercial HNO_3 for 2 weeks, which reveals a drastic change in reactivity as a consequence of trapping. Although the great resistance of the complex to decomposition could be considered very convenient for sensing purposes, what these observations are really showing is that the complex molecules are now trapped in sites that are inaccessible to the species in solution. The lack of changes in the absorption spectra of these samples upon treatment with NaN_3 solutions confirmed this conclusion.

The behavior of sonogels containing Cu−L complexes is quite different from that of the Cu−*tren* samples. In this case, hybrid materials of both series (A and B) remained colored and showed the spectrum typical of the binuclear Cu−L complexes after repeated washing. Treatment with an aqueous solution of NaN_3 changed the color in hours from blue to green, and the spectrum typical of $Cu_2L(N_3)^{3+}$ with a band centered at 440 nm

(35) Jain P. C.; Lingafelter, E. C. *J. Am. Chem. Soc.* **1967**, *89*, 6131.
(36) Cayley, G.; Cross, D.; Knowles, P. *J. Chem. Soc., Chem. Commun.* **1976**, 837.
(37) Powell, D. H.; Merbach, A. E.; Fábián, I.; Schindler, S.; Van Eldik, R. *Inorg. Chem.* **1994**, *33*, 4468.
(38) Basallote, M. G.; Martell, A. E. *Inorg. Chem.* **1988**, *27*, 4219.
(39) Basallote, M. G.; Durán, J.; Fernández-Trujillo, M. J.; Máñez, M. A. Unpublished work.

was obtained.[39] Although attack of these samples by concentrated acid leads to complete discoloration, the concentration of acid and the time required to complete the decomposition of the trapped complexes are both much larger than in solution. Thus, ca. 24 h are required to discolor a monolith in contact with a 1 M solution of HNO_3, whereas decomposition in solution at the same acid concentration is completed in a few milliseconds. In this respect, it has been pointed out that small species do not necessarily diffuse freely through the pore network of sol−gel materials and that the concentration of the solute inside the sonogel can be different from that in the external solution, especially in the case of ionic species.[16] In our case, the slowing of the reaction with H^+ is more severe than with the other reagents, which indicates that the problem cannot be simplified to diffusion barriers and that other effects must be considered. Thus, the surface of the pores can develop a certain positive charge during treatment with acid because of the interaction of H^+ ions with the silanol groups, which would lead to electrostatic repulsion with other protons in solution and to a smaller concentration of H^+ inside the sonogel network.

When acid-treated B-CuL sonogels were treated with Cu(II) solutions, the samples became slightly colored and showed spectra that suggested the presence of aqueous Cu(II) ions, although the color disappeared easily with washing. No evidence was obtained in any case of regeneration of Cu−L complexes trapped in this sol−gel material. These results clearly indicate that the Cu−L complexes are trapped in the B matrixes in sites accessible to external reagents (H^+, N_3^-) but the Cu^{2+}, LH_6^{6+}, and X^- ions are released into the solution once the complex decomposes.

In contrast, for acid-treated A-CuL samples, treatment with an aqueous solution of Cu(II) regenerates the initial spectra, although the concentration of the complex is lower. When the samples are then treated with NaN_3 solution, the spectrum changes to that of $Cu_2L(N_3)^{3+}$, which clearly indicates that the cryptand L remains trapped in the sol−gel material when the complex decomposes during treatment with acid. However, the amount of L trapped in the sol−gel structure decreases with successive treatments, and the cycle of reactions cannot be repeated more than three times.

As the results described above suggested that the pore network of the A-CuL samples allows the circulation of the smaller Cu^{2+}, N_3^-, and H^+ ions but hinders diffusion of the larger protonated cryptand, new samples (A-L) prepared from TEOS and $H_8L{\cdot}8HBr$ were studied. Despite the fact that the preparation of the sonogels was modified to allow for the preparation of suitable monolithic pieces, the results obtained in the chemical tests were very similar to those previously described for the A-CuL sonogels. Thus, Figure 1 shows the absorption spectra of (a) an initially washed sample, (b) the same sample after treatment with Cu(II) solution, and (c) the same sample after treatment with azide solution. The spectra show clearly that L is trapped in sites accessible to external reagents and suitable for the formation of the Cu−L and Cu−L−N_3^- complexes. The reference A sample without added cryptand simply traps aqueous Cu(II) and releases it rapidly upon washing. All attempts to trap L into the network from an external

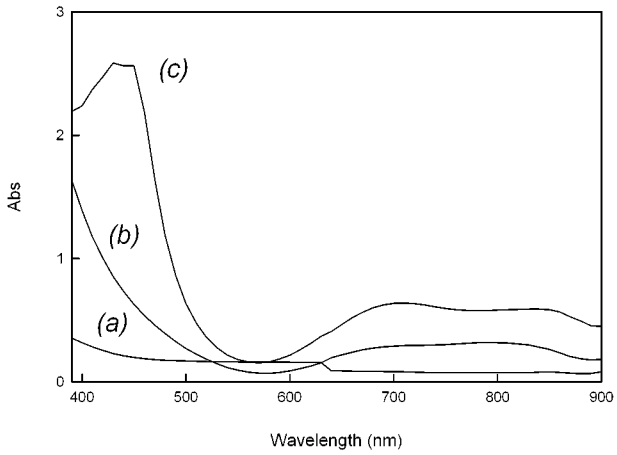

Figure 1. Absorption spectra corresponding to a monolithic sample of the A-L sonogel. Spectrum a corresponds to the sample after the initial washing protocol, spectrum b corresponds to the same sample after treatment with Cu^{2+} solution, and spectrum c was obtained after a new treatment with N_3^- solution.

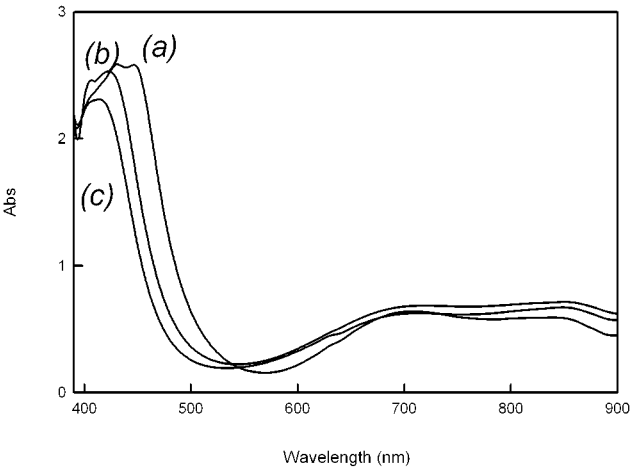

Figure 2. Effect of successive reaction cycles on the spectrum of an A-L sonogel treated with Cu(II) and N_3^-. Spectrum a is the same as in Figure 1c, and spectra b and c were obtained after (b) one and (c) two reaction cycles with H^+, Cu^{2+}, and N_3^-.

solution were unsuccessful, not only for the pure-silica sonogel (A sample), but also for all other samples. There is no case in which we have been able to increase the absorption signals corresponding to the trapped complexes by treatment of the xerogels with solutions containing the L ligand.

Figure 2 illustrates the effect of successive chemical treatments on A-L xerogels. Only the spectra corresponding to the stage of $Cu_2L(N_3)^{3+}$ formation are plotted, and they indicate that the concentration of trapped complex decreases with each reaction cycle. However, leaching of the cryptand is now less important than for the A-CuL samples, which allows more cycles with good absorption spectra. Nevertheless, as the number of cycles increases, there is also an increase in the time required to complete the color change for a given reaction. This is especially evident in the treatment with acid, where the complete loss of the band at ca. 440 nm after three reaction cycles was only achieved after treatment with concentrated HNO_3 (commercial acid diluted with the same volume of water) for 15 days. These results clearly indicate that the barrier to diffu-

sion increases with the number of chemical treatments carried out and suggests that the chemical reactions are accompanied by a substantial change in the pore network. It appears that the severe treatment with acid decreases the size of the pores and hinders diffusion of the ions. The displacement of the $Cu_2L(N_3)^{3+}$ band toward lower wavelength observed in Figure 2 is also probably a consequence of the changes in the pore network: if the pores became smaller, then the structure of the trapped complex could be conditioned to some extent by the surroundings, and small distortions from the structure in solution could lead to the observed displacement of the band. These small changes in the spectral properties of the added species upon trapping into the sol−gel network have been previously observed for other additives.[18,40]

As a summary, the reactivity data for the whole set of these new hybrid materials clearly indicate that the cryptand L and its binuclear Cu(II) complexes can be trapped into xerogel materials without the need to force covalent bonding of the ligand to the gel structure, although the actual behavior is strongly dependent on the nature of both the matrix and the added species. According to the reactivity behavior, up to three different types of sites can be distinguished. Sites of type a contain weakly trapped complex ions that are easily released upon washing. Sites of type b contain strongly trapped metal complex but are accessible to external reagents, which allows for the reversible reaction of the trapped complex with suitable reagents. Finally, sites of type c contain the metal complex trapped in an irreversible way because the sites are not accessible to an external solution. It is important to note that the channels connecting type b sites with the external solution allow for the easy, reversible transfer of small species such as Cu(II), N_3^-, and even *tren*, but they hinder the release to solution of the larger molecule of the cryptand L.

The types of sites created in the gel matrix appear to be determined by both the nature of the ligand or metal complex and the type of matrix. Hybrid materials prepared from the nonmacrocyclic Cu−*tren* complex mainly contain sites of types a (B matrix) and c (A matrix), but samples prepared from the binuclear Cu(II) cryptates also contain sites of type b. The appearance of sites of type a appears to be general, but sites of type b have been observed only for the A-CuL and A-L samples.

Whereas sites of types a and c are not useful for sensing purposes, sites of type b are very promising because the trapped complexes show a reactivity similar to that in solution, and so, predictions can be made from the comprehensive stability data available for these complexes. The slow kinetics of the reactions is caused, at least in part, by the use of monolithic samples. Actually, during the reaction of A-CuL and Cu(II)-treated A-L sonogels with azide, the color of the external parts of the monolith changes immediately to green, showing formation of $Cu_2L(N_3)^{3+}$, whereas the less-accessible central part retains the blue color complex for a long time. Thus, it appears that these diffusion problems can be easily overcome, or at least diminished, by the use of thinner monoliths or thin films.

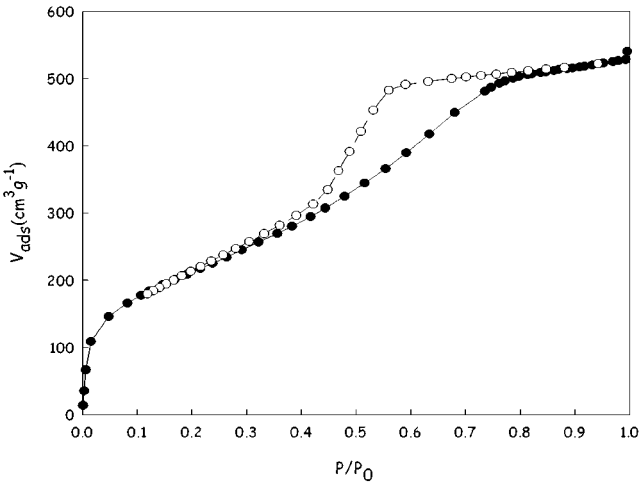

Figure 3. Nitrogen adsorption−desorption isotherm for an A-L sample showing a type IV shape according to the IUPAC classification.

Table 1. Summary of Textural Data for the Samples Discussed in This Work[a]

	surface area ($m^2\ g^{-1}$)			porous volume ($cm^3\ g^{-1}$)		pore size (nm)		
	S_{BET}	S_{micro}	S_{meso}	V_{pore}	V_{micro}	D_g	D_{DH}	D_{HK}
A-Cu*tren*	906	21	885	0.65	0.011	2.6	3.5	0.9
A-Cu−L	778	34	744	0.81	0.024	3.8	3.6	0.9
A	201	−	−	0.18	−	5.0	3.6	−
A−L	467	−	−	0.65	−	7.0	6.5	0.9
A-Lt	665	360	305	0.28	0.103	3.5	3.7	0.7

[a] Surface area and porous volume from BET (S_{BET}, V_{pore}) and t-test (S_{micro}, V_{micro}) methods and pore size from geometrical cylindrical model (D_g) and Dollimore−Heal (D_{DH}) and Horvath−Kawazoe (D_{HK}) Methods

Porosity Results. According to the reactivity data, the most promising samples for sensing purposes are those of the A series, and a detailed adsorption study was carried out for them. For all samples, the shape of the adsorption−desorption isotherms fit to the type IV IUPAC classification[41] with a hysteresis loop (Figure 3). From the isotherm analysis two main textural parameters are obtained: the specific pore volume V_{pore} (from the adsorption volume at saturation) and the specific surface area S_{BET} (from a fit to the BET equation in the lower relative pressure range).[42] In addition, if a cylindrical pore model is assumed, the ratio V/S provides an estimation of the mean pore size (D_g). The values of these textural parameters (Table 1) suggest that the larger binuclear molecule of the cryptate complex induces a more open structure for the xerogel network than the nonmacrocyclic mononuclear *tren* complex.

From the analysis of the gas volume adsorbed at increasing relative pressure, a distribution of the pore sizes in the sample can be inferred. This analysis is mainly based on the Kelvin equation for capillary condensation in the mesopores. It correlates the pore radius with the relative pressure when capillary condensation takes place at each pore size. The method of Dollimore and Heal was used to calculate the pore size

(40) Hartnett, A. M.; Ingersoll, C. M.; Baker, G. A.; Bright, F. V. *Anal. Chem.* **1999**, *71*, 1215.

(41) IUPAC Report on Physisorption Data for Gas/Solid Systems with Special Reference to the Determination of Surface Area and Porosity. *Pure Appl. Chem.* **1985**, *57*, 603.

(42) Brunauer, S.; Emmet, P. H.; Teller, E. *J. Am. Chem. Soc.* **1938**, *60*, 309.

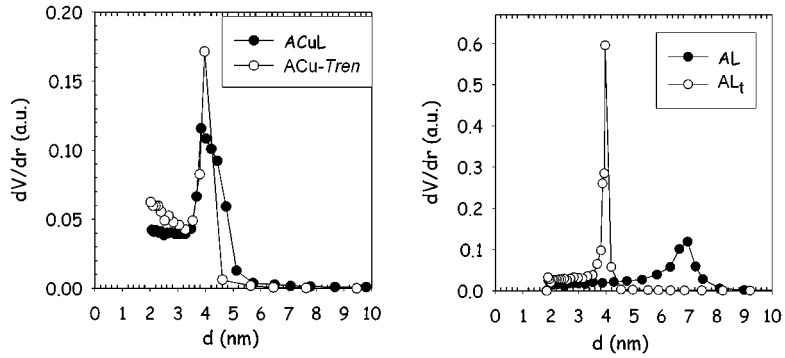

Figure 4. Dollimore-Heal pore size distribution for CuL and Cu−*tren* in (left) type A matrixes and (right) A-L and A-Lt sonogels.

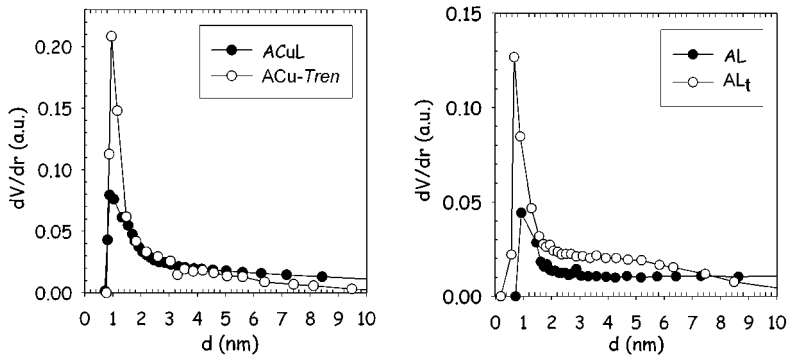

Figure 5. Horvath−Kawazoe pore size distribution for Cu−L and Cu−*tren* in (left) type A matrixes and (right) A-L and A-Lt sonogels.

(D_{DH}) using the Kelvin radius in a cylindrical pore model.[43] This method was applied to the desorption branch of the isotherms, and the results are shown in Figure 4. According to these results, the A-CuL and A-Cu*tren* samples each present a single maximum in their distributions centered on a diameter of 3.5 nm, with a strong decay for pore volumes associated with larger pore sizes that is sharper for the A-Cu*tren* sample. Xerogel materials can be considered as being made up of spherical particles, each in contact with two or more of its neighbors in a hierarchical structure.[44,45] The capillary condensation in this kind of solid can be explained by a simplified model in which the hysteresis is due to a different mechanism of filling and emptying of the crevices between contiguous spheres in the adsorption−desorption processes. The distribution of pore sizes in both samples suggests a large number of cavities of 3.5 nm between spheres.

However, the previously described pore structure does not justify the behavior of the complexes trapped in the two samples because these pore sizes are far from that required for the effective encapsulation of the complexes by the xerogel matrix. Actually, the size of the trapped Cu−L complexes must be close to that found in the crystal structure[28] of $[Cu_2L(\mu\text{-}CO_3)(H_3O)]Br_3{\cdot}3H_2O$, where the largest axis is only ca. 1.0 nm, the size of the Cu−*tren* complex being smaller.

Therefore, microporosity evidence was checked by the t-plot method,[46] and it was confirmed for both complex-doped samples. The micropore surface area and volume (S_{micro} and V_{micro}) were obtained for both samples from the slope and the *y*-intercept value of the t-plot, respectively, and the results in Table 1 reveal that the Cu−L complex induces a significantly higher micropore volume in the xerogel particles. To gain insight into the details of the micropore structure, an analysis of the micropore size using the Horvath and Kawazoe method[47] was also performed. This method avoids the Kelvin equation limitations in the micropore range, and it is suitable at the molecular range. The Horvath−Kawazoe distributions obtained for the A-CuL and A-Cu*tren* samples are displayed in Figure 5, and the micropore size values of the distribution maxima (D_{HK}) are also included in Table 1. For both complexes, there is a maximum at a diameter of 0.9 nm.

From a global analysis of the results in Table 1, both complex-doped xerogels can be depicted as aggregates of spherical particles with cavities of 3.5 nm, these particles having a certain microporosity with pores of 0.9 nm (Figure 6). In this schematic model, three potential positions for the guest molecule can be found: Type 1 positions would be those existing in the cavities between spheres, type 2 positions would be those located in the cavities inside the particles, and type 3 positions would be those completely trapped into the matrix. A comparison of this model with the conclusions derived from the reactivity behavior of the monoliths leads to equivalences between sites of types 1 and a, types 2 and b, and types 3 and c.

Type 1 sites are too large for enclosing purposes, and hence, when lodged in these sites, even the larger Cu−L−X species are released during the washing steps.

(43) Dollimore, D.; Heal, G. R. *J. Appl. Chem.* **1964**, *14*, 109.
(44) Zarzycki, J. *J. Non-Cryst. Solids* **1992**, *147−148*, 176.
(45) Rodríguez-Ortega, J.; Esquivias, L. *J. Sol-Gel Sci. Technol.* **1997**, *8*, 117.
(46) Mikhail, R. SH.; Brunauer, S.; Bodor, E. E. *J. Colloid Interface Sci.* **1968**, *26*, 54.
(47) Horváth, G.; Kawazoe, K. *J. Chem. Eng. Jpn.* **1983**, *16*, 470.

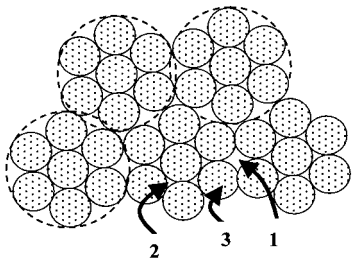

Figure 6. Hierarchical model for the sonogel matrixes; sites of type 1, 2 (between the aggregates), and 3 (closed into the matrix) are indicated. (See text.)

In contrast, molecules trapped in type 3 sites are not accessible for interaction with reagents in solution, and so, they remain irreversibly trapped. Finally, type 2 sites appear to be small enough to keep trapped species as large as the Cu−L complexes, but they allow the entry and exit of smaller species such as Cu^{2+}, H^+, and X^-. Thus, when a sonogel containing a Cu−L−X complex is treated with acid, decomposition according to eq 6 leads to the loss of Cu^{2+} and X^-, but L remains trapped as H_6L^{6+} ions. The fact that H_6L^{6+} ions remain trapped at these sites is fundamental for sensing purposes because it allows regeneration of the trapped complex by treatment with solutions containing Cu^{2+} and X^-. Moreover, because it is only the cryptand that remains trapped, following the treatment with acid, there is the possibility of substituting Cu^{2+} for a different cation such as Zn^{2+}, thus increasing the attractiveness of these systems for sensing. Actually, Fabrizzi and co-workers have reported several possibilities of sensing based on the use of L and related ligands.[25] More recently, the possibility of selective complexation of anions (NO_3^-, CrO_4^{2-}, $S_2O_3^{2-}$, etc.) by the protonated forms of L has been also reported.[26]

At this point, it is important to remember that A-CuL samples mainly contain complexes trapped at type 2 sites, whereas A-Cu*tren* only contain complexes at sites of type 3. These observations suggest that an effect on the network formation process is induced by the nature of the metal complex that determines the size of the micropores, the smaller Cu−*tren* species leading to a more closed structure. However, the Horvath−Kawazoe distributions reveal similar micropore sizes for both samples and suggest that the micropore size is independent of the size of the metal complex. Nevertheless, complexes trapped at the completely closed sites of type 3 do not appear in the Horvath−Kawazoe analysis, and so, the formation of the three types of sites is probably a consequence of the nature of the complex and the preparation conditions. In any case, the chemical behavior is clearly determined by the relative sizes of the cavities and the chemical species. The X-ray structures of salts of the L cryptand show a "Y" shape, with an internal cavity that can be described as a sphere of diameter 0.76 nm.[28] As the external dimensions are slightly higher, the size of the protonated ligand almost coincides with that of the micropores, which explains the difficulties encountered by H_6L^{6+} ions diffusing through the pore network from type 2 sites toward the outside of the monolith. As the size of the Cu−L complexes is slightly larger, the metal complex remains trapped. Following transformation of the Cu−L complexes into H_6L^{6+} by acid attack, diffusion of the protonated ligand through the pore network is possible because H_6L^{6+} (0.76 nm) is shorter than CuL (1.0 nm), which explains the gradual reduction of the absorption spectrum signals after each cycle of reactions. In contrast, the size of the trapped Cu−*tren* species is close to that found in the crystal structure[35] of [Cu(*tren*)(NCS)](SCN), and consideration of the cation as an sphere would lead to a diameter close to 0.4 nm, which allows for the easy release of these ions from type 2 sites.

Table 1 also includes textural data for the reference A and A-L samples. These xerogels show different porous structures because of the solvent substitution and higher pH used for their processing. Nevertheless, the effect of the L cryptand on the texture can be inferred from these samples, and the results show that its presence induces a higher porosity and a larger mean pore size in the xerogel matrix (see Figure 4). No evidence of microporosity is revealed by the t-tests of the A and A-L samples. However, the Howarth−Kawazoe analysis of the A-L sample leads to a micropore size (Table 1, Figure 5) similar to that of the A-CuL sample, which explains the similar behaviors of the two samples during the cycles of chemical reactions.

In addition, we have analyzed the textural modifications induced by several cycles of chemical reactions carried out inside the pore network (A-Lt sample). A comparison of textural data for the A-L and A-Lt samples reveals that the chemical reactions carried out on the A-L sample induce a decrease in both the porous volume and the pore size (Figure 4), which results in an increase in the surface area. In addition, substantial microporosity arises in the A-Lt sample (Figure 5), which strongly suggests a rearrangement of the xerogel pore network as a consequence of the chemical treatments. This rearrangement appears to consist of a reduction of the mesopore surface by the partial transformation of this space in the micropores, which must be accompanied of the partial release of the trapped ligand. It is also noticeable that the maximum of the Howard−Kawazoe distribution moves from 0.9 to 0.7 nm after several cycles of reaction. This new size of the type 2 cavities fits better to the H_6L^{6+} size and surely contributes to the more reversible behavior observed for this sample in comparison with the A-CuL samples. Moreover, the smaller size of the pores explains both the increased number of reaction cycles and the slower kinetics observed in the chemical tests.

Acknowledgment. Financial support by the Spanish Dirección General de Enseñanza Superior (Research Projects BQ2000-0232 and MAT 1998-0798) is gratefully acknowledged.

CM0111635